Role and mechanism of quercetin via the TLR4/MyD88/IRAK4 signaling pathway in the treatment of allergic rhinitis

CHENGLIN KANG[1,2], JIANGQI LIU[3], SHUQI QIU[3] and XUDONG WEI[1,2]

[1]The First School of Clinical Medicine, Lanzhou University, Lanzhou, Gansu 730000, P.R. China; [2]Department of Otolaryngology, Gansu Provincial Hospital, Lanzhou, Gansu 730000, P.R. China; [3]Department of Otolaryngology, Longgang E.N.T Hospital and Shenzhen Key Laboratory of Ear, Nose, Throat, Institute of Ear, Nose, Throat Shenzhen, Shenzhen, Guangdong 518172, P.R. China

Received February 4, 2026; Accepted May 6, 2026

DOI: 10.3892/etm.2026.13215

Abstract. Although quercetin has anti-allergic and anti-inflammatory properties, its role in allergic rhinitis (AR) and its potential molecular mechanism, especially whether it acts through the Toll-like receptor 4 (TLR4)/myeloid differentiation primary response 88 (MyD88)/interleukin-1 receptor-associated kinase 4 (IRAK4) signaling pathway, is currently unclear. Therefore, an ovalbumin (OVA)-induced AR mouse model was established to investigate whether quercetin can treat AR by regulating the TLR4/MyD88/IRAK4 signaling pathway. OVA and aluminum hydroxide were injected intraperitoneally for sensitization, and OVA was dripped into the nose to establish a mouse model of AR. The mice were scored on behaviors such as scratching, sneezing and a runny nose to assess the success of the modeling. The treatment groups were given the relevant drugs (dexamethasone and quercetin) by gavage for 1 week after successful modeling. Following the completion of treatment, the serum OVA-IgE, IL-4, IL-13, IL-1β, IL-17 and IL-10 levels were measured; changes in the nasal mucosa were observed; protein and mRNA expression levels of TLR4, MyD88, IRAK4 and NF-κB in lung tissue were determined; and changes in the percentages of regulatory T cells (Tregs) and T helper 17 (Th17) cells in the spleen were assessed. The results showed that compared with the normal control (NC) group, the allergic symptom scores were >10 points, and the serum levels of OVA-IgE, IL-4, IL-13, IL-1β and IL-17 increased, whereas the serum level of IL-10 decreased in the OVA group. Detachment and necrosis of the nasal mucosa, accompanied by tissue edema and inflammatory cell infiltration, were observed in the OVA group. Compared with the NC group, the relative expression mRNA and protein levels of TLR4, MyD88, IRAK4 and NF-κB in lung tissues increased, the percentage of Tregs decreased and the percentage of Th17 cells increased in splenocytes of the OVA group. Based on these results, it was hypothesized that quercetin inhibits inflammatory responses and induces immune tolerance by regulating the TLR4/MyD88/IRAK4 signaling pathway in a mouse model of AR.

Correspondence to: Professor Xudong Wei, The First School of Clinical Medicine, Lanzhou University, 222 Tianshui South Road, Chengguan, Lanzhou, Gansu 730000, P.R. China
E-mail: weixd93@lzu.edu.cn

Key words: quercetin, Toll-like receptor 4/myeloid differentiation primary response 88/interleukin-1 receptor-associated kinase 4 signaling pathway, inflammatory response, immune regulation, allergic rhinitis

Introduction

Atopic patients are a specific group of individuals who produce immunoglobulin E (IgE) antibodies in response to allergens in the environment. These patients often suffer from one or more atopic diseases, such as atopic dermatitis, asthma or allergic rhinitis (AR). When atopic patients inhale allergens, they develop AR, a non-infectious, chronic inflammatory disease of the nasal mucosa mediated primarily by IgE (1). AR has a high prevalence worldwide, reaching as high as 50% in some developed countries. It not only affects adults, but also children and adolescents (1). Although AR is not a serious disease, it can serve as the basis for several complications and is a major risk factor for patients with poorly controlled asthma. Statistically, perennial AR has no less impact on quality of life than asthma, but has notable negative consequences for the productivity of society as a whole (2,3). The prevalence of AR is rising globally due to factors such as increased urbanization, a decrease in the amount of time spent outdoors and the misuse of antibiotics. In addition, lifestyle changes, increased air pollution, fungi, infectious agents, tobacco, smog and other risk factors have increased the prevalence of AR, leading to its worsened impact (4). At present, the etiology of AR is not well understood, and there are no effective strategies to prevent the disease (5). The existing therapeutic options cannot completely cure the disease. Therefore, conducting more in-depth research into its pathogenesis and identifying new targets for preventing and treating AR are of notable importance.

Chemically known as 3,3',4',5,7-pentahydroxyflavone, quercetin (QUE), a naturally occurring flavonoid, is widely found in vegetables, fruits and medicinal herbs and has notable therapeutic potential, including anti-inflammatory, anticancer, antioxidant, neuroprotective, anti-allergic and antibacterial properties (6,7). QUE may serve a key role in AR treatment

by modulating multiple key targets (8,9). The T helper 1 (Th1)/Th2 immune cell imbalance can be regulated by QUE, which reduces IgE and histamine expression and inhibits the infiltration of eosinophils, macrophages and lymphocytes (10). Toll-like receptors (TLRs) are closely associated with innate immunity (3). The TLR4 signaling pathway can activate the downstream inflammatory NF-κB signaling pathway, leading to the release of inflammatory cytokines and chemokines (11). The inflammatory response can be markedly attenuated by inhibiting activation of the TLR4/NF-κB signaling pathway (12). In the present study, the aim was to explore the therapeutic effects of QUE on AR via the TLR4/myeloid differentiation primary response 88 (MyD88)/interleukin-1 receptor-associated kinase 4 (IRAK4) signaling pathway, and to investigate the effects of QUE on the inflammatory response and immune regulation in AR using a mouse model of AR.

Materials and methods

Reagents. In the present study, the following reagents were used: QUE (Puxi), dexamethasone (DEX; MilliporeSigma), ovalbumin (OVA; MilliporeSigma; grade III), TLR4 and MyD88 (cat. nos. AF8187 and AF7524, respectively; Beyotime Biotechnology), NF-κB p65 (cat. no. 8242; Cell Signaling Technology, Inc.), IRAK4 (cat. no. ab119942, Abcam), BCA kit (Thermo Fisher Scientific, Inc.), SYBR Green qPCR Master Mix and RT Master Mix for quantitative PCR (qPCR; MedChemExpress), ELISA kit OVA-IgE (cat. no. MOFI01017; Assay Genie), mouse IL-17 ELISA Kit (cat. no. CSB-E04608m; Cusabio Technology, LLC), mouse IL-1β ELISA Kit, mouse IL-10 ELISA Kit, mouse IL-13 ELISA Kit, mouse IL-4 ELISA Kit (cat. nos. 1210122, 1211002, 1211302 and 1210402, respectively; all Dakwei), Flow-through antibody FITC Rat anti-mouse CD4 antibody, APC Rat anti-mouse CD25 antibody, PerCP Rat anti-mouse FOXP3 antibody (cat. nos. 553055, 552880 and 563902; all BD Biosciences) and Cell Fixation Membrane Breaker (eBioscience; Thermo Fisher Scientific, Inc.).

Experimental instruments. The following instruments were used in the present study: SDS-PAGE electrophoresis system, western blot transfer system, ChemiDoc MP multifunctional chemiluminescence imaging system (all Bio-Rad Laboratories, Inc.), BD FACSCanto II flow cytometer (BD Biosciences), Enzyme labeler SpectraMax Paradigm MultiMode Microplate Reader (Molecular Devices, LLC).

Animal study. In the present study, a total of 72 female BALB/c mice aged 4-6 weeks old were purchased from the Guangdong Experimental Animal Center [animal use license no. SCXK (Guangdong) 2022-0002; certificate of conformity no. 44007200114118]. The mice were housed in an air-conditioned animal room (temperature, 25±1˚C; humidity, 65±5%) for 1 week to allow them to acclimate. The present study was performed in accordance with the ARRIVE guidelines for animal research and complied with all relevant regulations. All experimental protocols used in the present study complied with animal ethics standards and were approved by the Experimental Animal Ethics Committee of Shenzhen Longgang E.N.T Hospital (approval no. 2022-0426). All efforts were made to minimize animal suffering. All animals were euthanized in accordance with the approved protocol at the end of the experiment. No unexpected deaths were observed, and no premature euthanasia procedures were carried out during the entire study period. Premature euthanasia procedures would be initiated if any of the following conditions occurred: Animals are unable to feed themselves, suffer from severe dehydration, severe infection, a moribund state, respiratory distress or cyanosis.

Establishment of the animal model. Previous studies have shown that female sex hormones increase the likelihood of developing AR and exacerbate eosinophilic inflammation in the nasal mucosa (13-15). Therefore, a mouse model of AR was established using female BALB/c mice. The mice were randomly assigned to one of four groups: Normal control (NC), OVA, DEX and QUE, with 6 mice per group. A total of 24 mice were used in each independent repeated experiment, and 3 independent repeated animal experiments were conducted. Except for the NC group, the remaining groups were sensitized with 200 μl sensitization working solution [containing 2 mg $Al(OH)_3$ and 100 μg OVA] by intraperitoneal injection on days 0, 7 and 14 for basal sensitization, and challenged on day 21 by nasal drip (10 μl per nostril) with OVA dissolved in saline (10 μg/μl) once daily for 7 days. The treatment of the NC group was replaced with normal saline, and mice were treated using the same methodology.

Behavioral assessment. The mouse model was expected to show symptoms such as sneezing, rubbing, face scratching and a runny nose after a successful challenge; the success of the model was assessed by observing these symptoms. On the final day of the 7-day challenge, the behavioral assessment was initiated within 30 min of completion. Allergy symptoms (such as sneezing, scratching and a runny nose) were scored after the challenge, and the observation period lasted 30 min. Scoring was performed based on the criteria outlined in Table I. The total score was recorded using the superposition method, and a score of >5 was considered successful modeling.

Treatment of animal models. The treatment groups (DEX and QUE) received 10 mg/kg DEX or 50 mg/kg QUE by gavage in the afternoon of the day of challenge, after successful modeling, once daily for 7 days. The NC and OVA groups were treated by gavage with equal amounts of saline. Mice in all groups were further sensitized with nasal drops as before, and their behavioral changes were observed during the 7 days of treatment. Efficacy was evaluated by analyzing symptom scores in each group during the treatment period. The mice were anesthetized with isoflurane on day 35 (5% induction and 2% maintenance). Once the mice completely lost the ability to right themselves, their respiratory rate markedly decreased or they showed no response to painful stimuli, they were euthanized by cervical dislocation. Subsequently, blood from the eye, nose, lungs and spleen was collected for subsequent analysis (Fig. 1).

ELISA-based detection of OVA-IgE, IL-4, IL-13, IL-1β, IL-17 and IL-10 in the serum of mice. Blood from the eye was collected, left at room temperature for 30 min, then centrifuged

Table I. Criteria for scoring allergic symptoms in ovalbumin-induced mouse model.

Biological scoring	Scratching	Sneezing	Runny nose
0	None	None	None
1	Occasionally (1-2 times)	1-3	Flow to anterior nostril
2	Frequently	4-10	Beyond the anterior nostril
3	Scratching incessantly	>10	Runny nose all over the face

Table II. Quantitative PCR primer sequences.

Genes	Primer sequences (5'-3')
TLR4-F	ATGGCATGGCTTACACCACC
TLR4-R	GAGGCCAATTTTGTCTCCACA
MyD88-F	TCATGTTCTCCATACCCTTGGT
MyD88-R	AAACTGCGAGTGGGGTCAG
IRAK4-F	CATACGCAACCTTAATGTGGGG
IRAK4-R	GGAACTGATTGTATCTGTCGTCG
NF-κB-F	ATGGCAGACGATGATCCCTAC
NF-κB-R	TGTTGACAGTGGTATTTCTGGTG
GAPDH-F	AGGTCGGTGTGAACGGATTTG
GAPDH-R	TGTAGACCATGTAGTTGAGGTCA

F, forward; R, reverse; TLR4, Toll-like receptor 4; MyD88, myeloid differentiation primary response 88; IRAK4, interleukin-1 receptor-associated kinase 4.

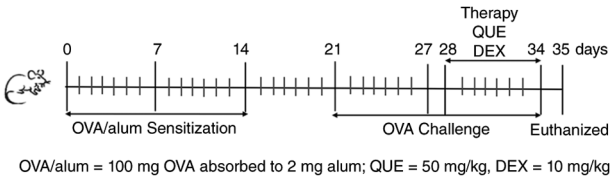

Figure 1. Schematic diagram of the animal modeling. OVA, ovalbumin; QUE, quercetin; DEX, dexamethasone; alum, aluminum hydroxide.

at 12,880 x g for 10 min at 4˚C to isolate the upper serum layer, which was stored at -80˚C until further use. The serum levels of OVA-IgE, IL-4, IL-13, IL-17, IL-1β and IL-10 in mice were measured using ELISAs according to the manufacturer's protocol.

Histopathological analysis by hematoxylin-eosin (HE) staining. The nasal tissues of mice were isolated intact under aseptic conditions, the surface blood was washed, and the tissues were stored in EP tubes containing 4% paraformaldehyde for fixation at room temperature for 24 h. After decalcification, dehydration, transparency, wax immersion and embedding, the sections were cut into 5-μm-thick slices. Then the sections were stained with HE solution at room temperature for 3 min after spreading, baking, dewaxing and rehydrating. After dehydration, clearing and drying, the slides were sealed and finally observed under a brightfield microscope.

Reverse transcription (RT)-qPCR. Total RNA was isolated from mouse lung tissue using TRIzol®, and RNA concentration and purity were determined. According to the RT Master Mix for qPCR (gDNA digest plus) kit instructions, the total RNA was reverse transcribed into cDNA with a final transcription volume of 20 μl. TLR4, MyD88, IRAK4, NF-κB p65 and GAPDH primers were synthesized by Sangon Biotech Co., Ltd. (Table II). qPCR amplification was performed according to the instructions of SYBR Green qPCR Master Mix (Low ROX) kit under the following thermocycling conditions: Initial hold at 95˚C for 5 min, followed by 40 cycles of denaturation at 95˚C for 10 sec and annealing at 60˚C for 30 sec. The relative mRNA expression levels in each group were calculated using the $2^{-\Delta\Delta Cq}$ method based on the reference (16).

Western blot. Mice lung tissues were collected under aseptic conditions, stripped of surrounding fat, blood vessels and connective tissue and stored at -80˚C. When required, tissues were thawed to room temperature and washed 3 times with PBS. Subsequently, the protein lysis solution with protease inhibitor was added. The lysis solution was prepared by mixing RIPA lysis buffer (strong; cat. no. P0013B; Beyotime Biotechnology) with PMSF protease inhibitor (cat. no. 36978; Thermo Fisher Scientific, Inc.) at a volume ratio of 100:1. The tissues were ground and further lysed for 30 min at 4˚C. The lysates were then centrifuged at 4˚C at 12,880 x g for 10 min. The supernatant was collected as a protein stock solution. Protein concentration was measured using a BCA kit. After adjusting the protein concentration of each group to the same level, 30 μg protein was loaded per lane for SDS-PAGE electrophoresis using a 5% loading gel and a 12% resolving gel, at 80 V during the loading gel and at 120 V during the resolving gel. Subsequently, the proteins were transferred to PVDF membranes, blocked with TBST (0.1% Tween-20) containing 5% skim milk powder for 1 h. The membranes were cut according to the location of the protein of interest and incubated with primary antibodies overnight at 4˚C on a shaker at the following dilutions: GAPDH (1:2,000; cat. no. MA5-15738-A488; Thermo Fisher Scientific, Inc.), TLR4 (1:2,000; cat. no. AF8187; Beyotime Biotechnology), NF-κB p65 (1:1,000; cat. no. 8242; Cell Signaling Technology, Inc.), IRAK4 (1:1,000; cat. no. ab119942; Abcam), and MyD88 (1:1,000; cat. no. AF7524; Beyotime Biotechnology). The following day, membranes were rewarmed at room temperature for 1 h, washed three times with TBST (10 min per wash), incubated with goat anti-rabbit IgG antibody (1:5,000; cat. no. ab6728; Abcam) for 2 h, washed three times again with TBST (10 min per wash), and developed using the SuperSignal™ West Femto Chemiluminescent Substrate (cat.

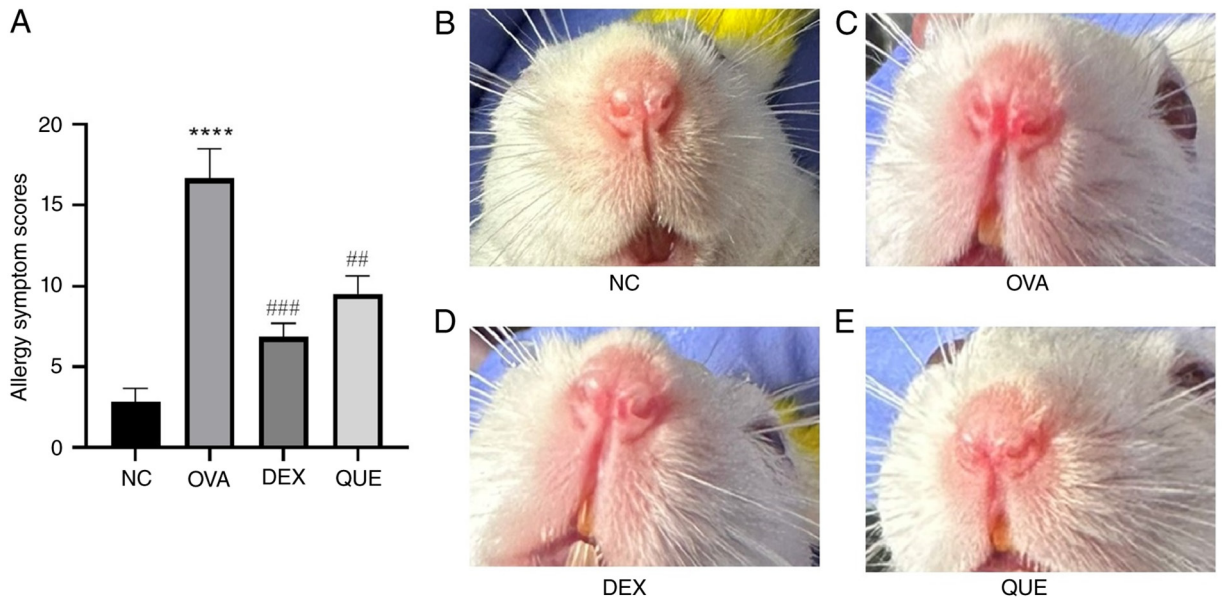

Figure 2. Allergy symptom scores and local nasal mucosal manifestations in mice (n=6 per group). (A) Allergic symptom scores in mice on day 34. Local nasal manifestations of mice in the (B) NC, (C) OVA, (D) DEX and (E) QUE groups on day 34. Data are presented as the mean ± SEM. ****P<0.0001 vs. NC; $^{##}$P<0.01, $^{###}$P<0.001 vs. OVA. NC, normal control; OVA, ovalbumin; Dex, dexamethasone; QUE, quercetin.

no. 34098CN; Thermo Fisher Scientific, Inc.). The results were analyzed using ImageJ (version 1.54g; National Institutes of Health).

Flow cytometry for detection of Tregs and Th17 cells in splenocytes. After euthanasia of the mice, the spleen was aseptically stripped, ground in a flat dish containing PBS, filtered and washed with PBS, Subsequently, 300 μl erythrocyte lysate was added, the samples were shaken and mixed, and incubated at 4˚C for 5 min. Next, the splenocytes were then divided into two halves; one half was used to assess Tregs, and the other half to assess Th17 cells. Blank control tubes, control isotype tubes, CD4 and CD25 single-stained tubes, and CD4 and IL-17 single-stained tubes were set up separately. A total of 1 μl of undiluted CD4 antibody and 1 μl of undiluted CD25 antibody was added to each tube of the Tregs assay; 1 μl of undiluted CD4 antibody was added to each tube for the Th17 cells assay, and all the samples were incubated for 30 min in the dark at 4˚C, and then 400 μl fixation buffer was added and cell were fixed for 1 h at 4˚C. A total of 1 μl of undiluted FOXP3 antibody and 300 μl permeabilization buffer were added to each tube of the Treg cells assay; 2 μl of undiluted IL-17 antibody and 300 μl permeabilization buffer were added to each tube of the Th17 cells assay. All the samples were shaken thoroughly, incubated overnight at 4˚C, washed twice with PBS and then evaluated using a BD FACSCanto II flow cytometer (BD Biosciences). The number of cells per sample was set to 50,000-100,000 for flow cytometry, and cellular debris and dead cells were excluded. Data analysis was performed using FlowJo software (version 7.6.1_Min; FlowJo LLC; BD Biosciences).

Statistical analysis. Data were analyzed and plotted using Graph Pad Prism version 8.0 (Dotmatics), and data are presented as the mean ± standard deviation. A one-way ANOVA was used for comparison between multiple groups, followed by Tukey's post hoc test for multiple comparisons. P<0.05 was considered to indicate a statistically significant difference.

Results

Allergic symptom score in the OVA-induced mouse model. The mice in the NC group occasionally had scratchy noses, while the mice in the AR model group had notable symptoms, including a scratchy nose, sneezing and a runny nose, and all scores were >10, indicating the successful establishment of the model. During the treatment of mice after successful modeling, the nasal drip was continued as before until the day before the mice were sacrificed (days 28-34); it was noted that the allergic symptoms persisted in the OVA group during these 7 days, whereas the scratching, runny nose and rubbing symptoms of the mice in the treatment groups (DEX and QUE groups) decreased daily in comparison with the OVA group, as assessed daily according to the scoring criteria in Table I. Finally, the results showed that the OVA group allergy symptom scores were significantly higher than those of the NC group (P<0.0001). The symptoms were significantly reduced in the DEX (P<0.001) and QUE (P<0.01) groups compared with those in the OVA group after treatment, and there was no notable change in the nasal symptoms in the NC group (Fig. 2A). Under microscopic examination of HE-stained sections, the nasal mucosa of the OVA group appeared more congested than that of the NC group, and after treatment the congestion appeared reduced in the DEX and QUE groups (representative images shown in Fig. 2B-E, which only partially reflect the differences observed by the naked eye).

OVA-IgE, IL-4, IL-13, IL-17, IL-1β and IL-10 expression levels in the serum of mice. OVA-IgE, IL-4, IL-13, IL-17, IL-1β and IL-10 levels in mouse serum at different time

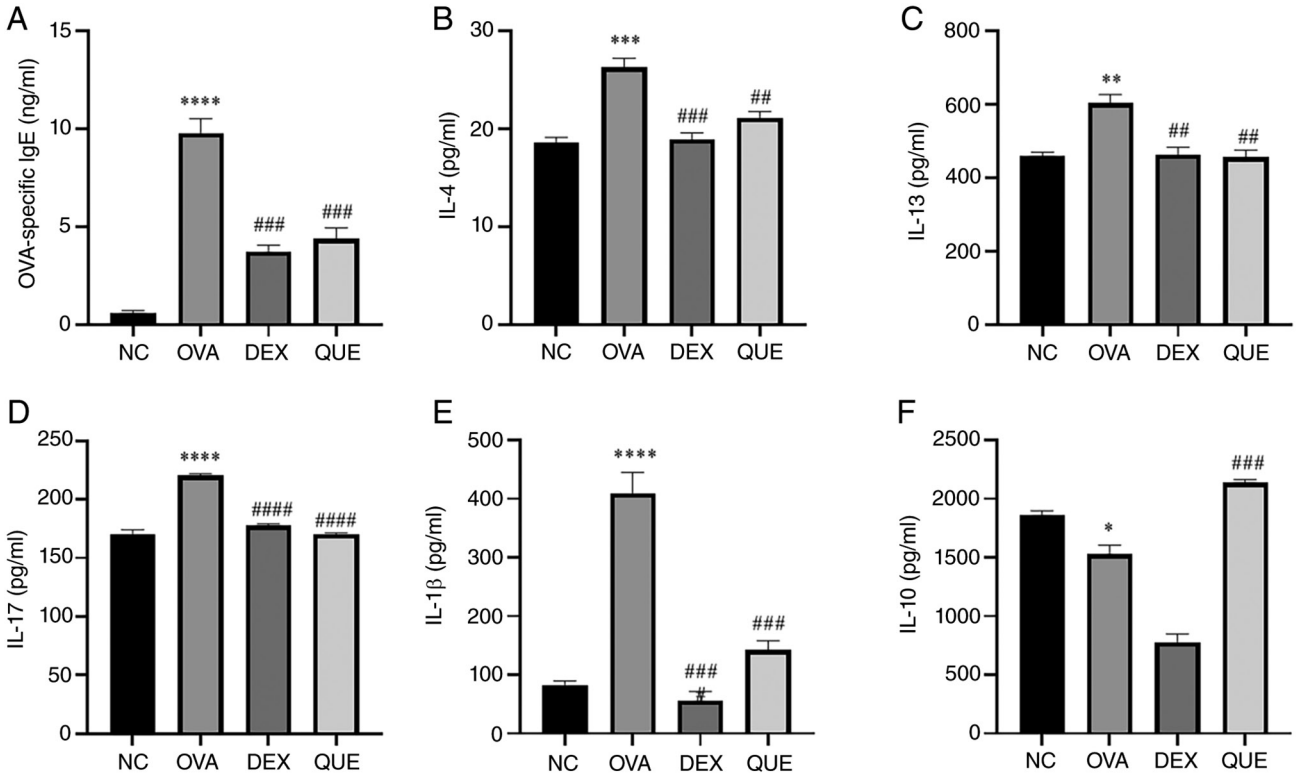

Figure 3. Production of OVA-IgE, IL-4, IL-13, IL-17, IL-1β and IL-10 in the serum of mice. (A-F) Results of OVA-IgE, IL-4, IL-13, IL-17, IL-1β and IL-10 relative secretion levels in NC, OVA, DEX and QUE groups. Data are presented as the mean ± SEM. *P<0.05, **P<0.01, ***P<0.001, ****P<0.0001 vs. NC; $^{\#\#}$P<0.01, $^{\#\#\#}$P<0.001, $^{\#\#\#\#}$P<0.0001 vs. OVA. NC, normal control; OVA, ovalbumin; DEX, dexamethasone; QUE, quercetin.

points were assessed using ELISA. The results showed that OVA-IgE, IL-4, IL-13, IL-17 and IL-1β levels increased in the OVA group compared with the NC group and decreased in the DEX and QUE groups compared with the OVA group. This indicates that OVA increased the serum levels of OVA-IgE, IL-4, IL-13, IL-17 and IL-1β in mice, and QUE reversed the OVA-induced changes. For IL-10, its expression was decreased in the OVA group compared with the NC and increased in the QUE group compared with the OVA group. This suggests that QUE reversed OVA-induced changes in IL-10 levels (Fig. 3).

HE staining of the histopathological changes of the nasal mucosa in mice. The HE-stained sections of the nasal cavity showed that the nasal mucosa of the NC group was generally intact, with an intact epithelial structure; the glandular cell morphology was neat and orderly, with relatively little inflammatory cell infiltration and no obvious exudation. In the OVA group, the nasal mucosa was incomplete, with notable mucosal disruption, shedding, necrosis, tissue edema, small vessel dilatation, glandular hyperplasia, disorganized arrangement of glandular cells and obvious infiltration of inflammatory cells. In the DEX and QUE groups, mucosal morphology improved, with mucosal damage, shedding and necrosis all reduced; glandular hyperplasia was reduced, and glandular cell arrangement tended to be orderly; inflammatory cell infiltration was reduced; and tissue edema was reduced compared with that in the OVA group (Fig. 4).

Effect of QUE on the mRNA expression levels of TLR4, MyD88, IRAK4 and NF-κB. The mRNA expression levels of TLR4, MyD88, IRAK4 and NF-κB in the lungs of mice were measured using qPCR. The results showed that the expression of TLR4, MyD88, IRAK4 and NF-κB was increased in the OVA group compared with the NC group, and decreased in the DEX and QUE groups compared with the OVA group. Thus, QUE reversed the OVA-induced effects on the aforementioned mRNAs (Fig. 5).

Effect of QUE on the protein expression levels of TLR4, MyD88, IRAK4 and NF-κB. The relative expression levels of TLR4, MyD88, IRAK4 and NF-κB proteins in the lungs of mice were assessed using western blotting. The relative expression levels of these proteins were significantly increased in the OVA group compared with the NC, and reduced in the DEX and QUE groups compared with the OVA group. This indicates that QUE inhibited protein expression of members of the TLR4/MyD88/IRAK4 signaling pathway (Fig. 6).

Effect of QUE on the percentage of Treg and Th17 cells in splenocytes. The percentages of Tregs ($CD4^+/CD25^+/FOXP3^+$) and Th17 ($CD4^+$/IL-17) cells in mouse splenocytes were assessed using flow cytometry. The results showed that the percentage of Tregs decreased in the OVA group compared with the NC group, and increased in the DEX and QUE groups compared with the OVA group (Fig. 7A-E). This suggests that OVA reduced the number of Tregs in splenocytes, whereas DEX and QUE reversed the OVA-induced reduction in Tregs and potentially promoted Treg differentiation and proliferation. Additionally, the results showed that the percentage of Th17 cells increased in the OVA group compared with the NC group, and decreased in the DEX and QUE groups compared with the OVA group (Fig. 7F-J). This indicates that OVA

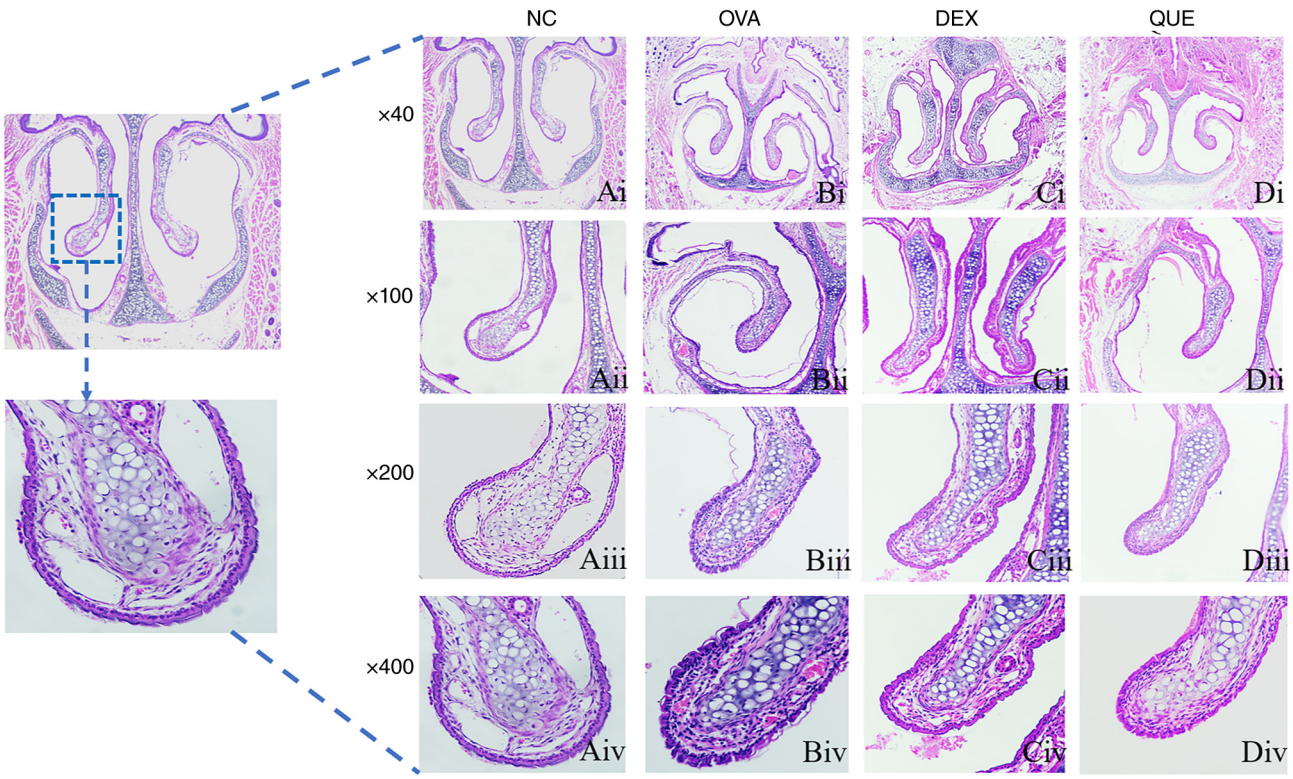

Figure 4. Histopathological hematoxylin-eosin-stained sections of the mouse nasal mucosa. Histopathological sections of stained tissues from the (Ai) NC, (Bi) OVA, (Ci) DEX and (Di) QUE groups; magnification, x40. Histopathological sections of stained tissues from the (Aii) NC, (Bii) OVA, (Cii) DEX and (Dii) QUE groups; magnification, x100. Histopathological sections of stained tissues from the (Aiii) NC, (Biii) OVA, (Ciii) DEX and (Diii) QUE groups; magnification, x200. Histopathological sections of stained tissues from the (Aiv) NC, (Biv) OVA, (Civ) DEX and (Div) QUE groups; magnification, x400. NC, normal control; OVA, ovalbumin; DEX, dexamethasone; QUE, quercetin.

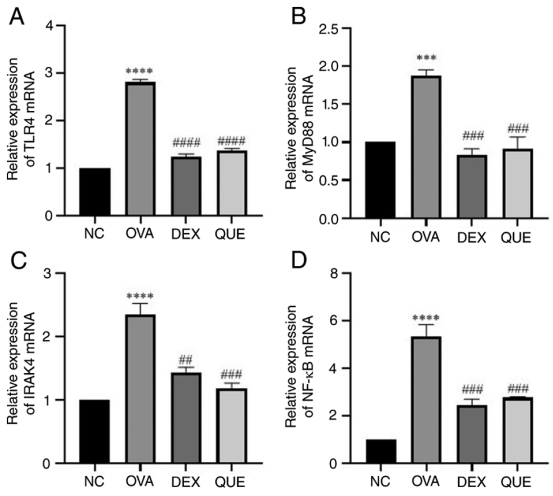

Figure 5. Effect of QUE on mRNA of TLR4, MyD88, IRAK4 and NF-κB. Results of (A) TLR4, (B) MyD88, (C) IRAK4 and (D) NF-κB mRNA relative expression levels in NC, OVA, DEX and QUE groups. Data are presented as the mean ± SEM of three repeats. ***P<0.001, ****P<0.0001 vs. NC; $^{##}$P<0.01, $^{###}$P<0.001, $^{####}$P<0.0001 vs. OVA. NC, normal control; OVA, ovalbumin; DEX, dexamethasone; QUE, quercetin; TLR4, Toll-like receptor 4; MyD88, myeloid differentiation primary response 88; IRAK4, interleukin-1 receptor-associated kinase 4.

increased the percentage of Th17 in splenocytes, whereas DEX and QUE reversed the OVA-induced increase in the percentage of Th17 cells.

Discussion

The primary clinical symptoms of AR include an itchy nose, runny nose and sneezing. Examination can reveal pale edema of the nasal mucosa, clear water-like secretions in the nasal cavity and hyperemia of the nasal mucosa in the acute phase. QUE can alleviate allergic symptoms in the nasal mucosa by reducing the levels of angiogenic factors and inhibiting oxidative stress (17,18). In the present study, BALB/c mice exhibited notable nasal scratching after successful modeling, suggesting they may have experienced nasal itching. Repeated nose scratching can lead to whisker loss and thinning of the fur around the nose in OVA-induced mice, and these manifestations were observed in the present study post-modeling. At the same time, it was observed that the allergic symptoms in the QUE and DEX groups gradually decreased over 7 days of treatment compared with the OVA group. This indicates that QUE alleviated the OVA-induced allergic symptoms in mice, and its effects were similar to those of DEX. It was also observed that the nasal mucosa of the OVA-induced mice model was more congested than that of the NC group, indicating that the inflammation was in the acute phase. This also shows that the modeling was successful. Scratching and rubbing were markedly reduced in the DEX and QUE groups after treatment, and congestion of the nasal mucosa was improved compared with that of the OVA group. This indicates that QUE alleviated nasal itching and nasal mucosal congestion in mice with AR. From this perspective,

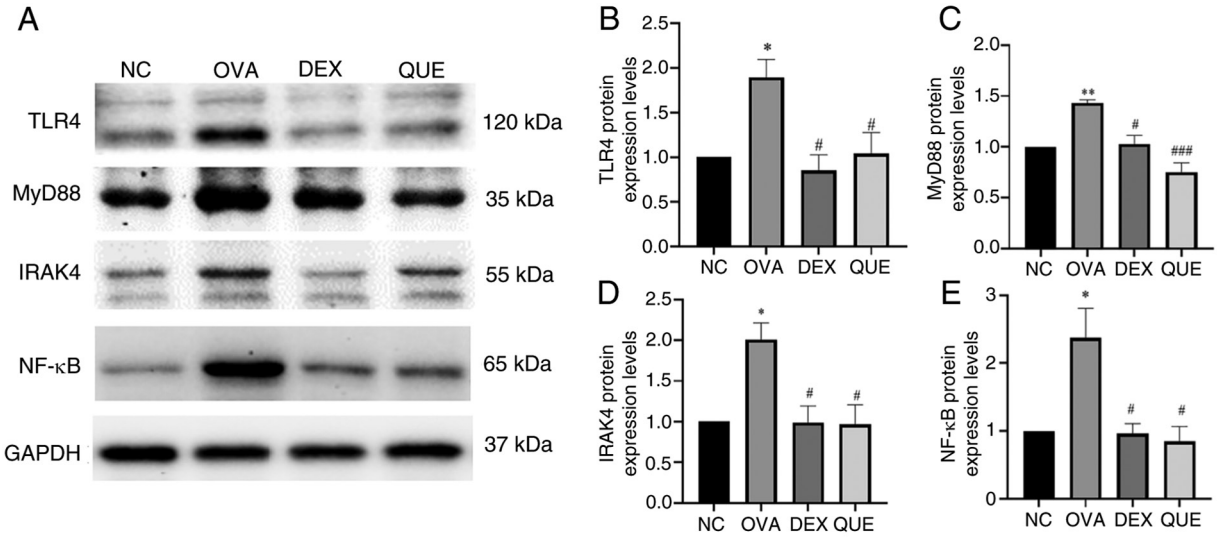

Figure 6. Effects of QUE on TLR4, MyD88, IRAK4 and NF-κB protein levels. (A) A significant increase was observed in the relative expression of TLR4, MyD88, IRAK4 and NF-κB proteins in the OVA group compared with the NC group. The relative expression of these proteins was lower in the DEX and QUE groups than in the OVA group. Semi-quantification of (B) TLR4, (C) MyD88, (D) IRAK4 and (E) NF-κB protein expression levels. Data are presented as the mean ± SEM of three repeats. *P<0.05, **P<0.01 vs. NC; $^{\#}$P<0.05, $^{\#\#\#}$P<0.001 vs. OVA. NC, normal control; OVA, ovalbumin; DEX, dexamethasone; QUE, quercetin; TLR4, Toll-like receptor 4; MyD88, myeloid differentiation primary response 88; IRAK4, interleukin-1 receptor-associated kinase 4.

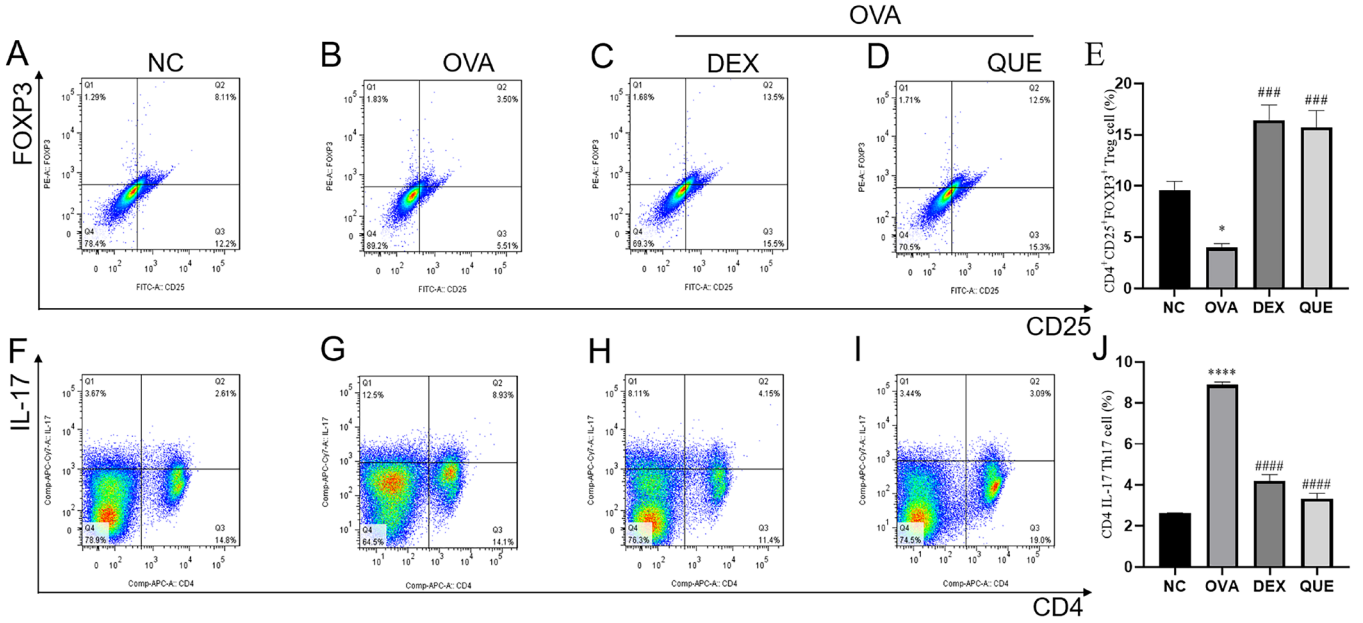

Figure 7. Percentage of Tregs and Th17 cells in splenocytes of mice. Percentage of Tregs in the splenocytes of mice in the (A) NC, (B) OVA, (C) DEX and (D) QUE groups. (E) Statistical analysis of the percentage of Tregs. Percentage of Th17 cells in splenocytes of mice in (F) NC, (G) OVA, (H) DEX and (I) QUE groups. (J) Statistical analysis of the percentage of Th17 cells. Data are presented as the mean ± SEM of three repeats. *P<0.05, ****P<0.0001 vs. NC; $^{\#\#\#}$P<0.001, $^{\#\#\#\#}$P<0.0001 vs. OVA. NC, normal control; OVA, ovalbumin; DEX, dexamethasone; QUE, quercetin; Th17, T helper 17; Treg, regulatory T cell.

the treatment was effective. For the treatment groups that did not fully return to normal levels, it was hypothesized that this may be due to insufficient treatment time or individual differences in dosage performance, but further research is required. The symptoms of AR are caused by allergic inflammatory mediators released when allergens enter the body and stimulate the nasal mucosa. Re-exposure of sensitized individuals to the same allergen activates and degranulates mast cells and basophils, which release histamine, leukotrienes, prostaglandins and other inflammatory mediators, leading to acute AR symptoms (1,19). In the present study, a mouse model of AR was induced by intranasal OVA challenge to evaluate whether treatment with QUE could alleviate allergic symptoms. Although the levels of histamine, leukotrienes and prostaglandins were not directly measured in this study, the reduction in sneezing, scratching and nasal congestion in the treatment group indirectly suggests that QUE may have influenced the release of these mediators.

IL-17 is primarily produced by Th17 cells and is often elevated in AR (20). This was also demonstrated by the ELISA results, which were consistent with the flow cytometry findings. IL-1β is a key cytokine that promotes AR (21). IL-1β activates the NF-κB pathway, promoting IL-13 production (22). IL-4 and IL-13 contribute to the production of mucus and IgE, thereby releasing pro-inflammatory mediators that, in turn, promote the development of allergic reactions (23). IL-10 serves multiple roles in immune regulation and inflammation, and its deficiency is associated with increased IgE in AR (24). The immunomodulatory effect of QUE was characterized by reductions in IL-4, IL-5, IL-13, IL-1β, TNF-α and IgE levels (25). The results of the present study showed that OVA-specific IgE, IL-4 and IL-13 levels were increased and IL-10 levels were decreased in the serum of the OVA-induced mouse model, and that these indicators were reversed after QUE and DEX treatment. The increase of OVA-specific IgE in the OVA group may be associated with the increase of IL-13, IL-4 and IL-1β and the decrease of IL-10. The mechanism is that IL-4 and IL-13 promote IgE production, whereas IL-10 suppresses IgE production, and IL-1β enhances the Th2-type inflammatory response. Therefore, increased IL-4, IL-13, IL-1β together with decreased IL-10 result in higher OVA-specific IgE levels. It is necessary to conduct more in-depth research into their relationship in subsequent experiments.

QUE, with the anti-allergic function of inhibiting the production of histamine and pro-inflammatory mediators, can regulate the stability of the Th1/Th2 balance, reduce antigen-specific IgE antibodies released by B cells and decrease IL-4 in serum, thereby reducing allergic airway inflammation and airway hyperresponsiveness (26). QUE can also reduce $Ca2^{+}$ influx induced by allergy and inhibit chemokine release, similar to the mast cell stabilizer DEX (27). In allergic conditions, the activation of innate and adaptive immunity can be attenuated by QUE (10). In the treatment groups (DEX and QUE), IL-4 and IL-13 levels were lower than in the OVA group, suggesting that QUE reduced OVA-induced IL-4 and IL-13 levels and that the reduction of IL-4 and IL-13 may further reduce IgE. This also suggests that blocking the production of IL-4 and IL-13 can treat AR and further verifies the anti-inflammatory and anti-allergic effects of QUE.

The nasal mucosa is rich in small blood vessels. When allergens trigger an allergic response, inflammatory mediators cause congestion and edema of the submucosal tissue, smooth muscle contraction, increased vascular permeability and mucus secretion. These inflammatory mediators can also increase the number of eosinophils deep in the nasal mucosa, and excessive accumulation of eosinophils further releases toxic proteins that can damage the integrity of respiratory epithelial cells (28,29). Under the synergistic effect of chemokines, inflammatory cells infiltrate the nasal mucosal tissue, triggering inflammatory responses that further damage the nasal mucosal tissue and lead to clinical symptoms (1). The infiltration of inflammatory cells in the nasal mucosa tissues of mice with chronic sinusitis or AR can be alleviated by QUE (8,30). Ke *et al* (31) showed that QUE alleviated OVA-induced thickening of the nasal mucosa and increased eosinophils in the nasal cavity in an OVA-induced mouse model of AR. Although the study by Ke *et al* (31) has demonstrated the anti-allergic effects of QUE in a similar mouse model, the present study focuses on the differentiation balance between Th1/Th2 and Treg/Th17 cells. It systematically reveals the regulatory role of QUE in modulating the Treg/Th17 balance via the TLR4/MyD88/IRAK4 signaling pathway in an OVA-induced AR mouse model, thereby expanding the understanding of the molecular targets of QUE in the treatment of AR. In the present study, the HE staining results showed that the nasal mucosa in the OVA group exhibited notable disruption, shedding and necrosis; dilated submucosal small blood vessels; glandular hyperplasia; disordered glandular cell arrangement; and infiltration of inflammatory cells. After treatment, the integrity of the nasal mucosa was partially restored, tissue edema was alleviated, the arrangement of glandular cells tended to be more orderly and the number of infiltrating inflammatory cells was reduced compared with the OVA group. The number of inflammatory cells in the nasal mucosa differed markedly. From a morphological perspective, QUE improved mucosal morphology, reduced the number of inflammatory cells and restored the integrity of the nasal mucosal epithelium in the OVA-induced mice model. This further demonstrates the anti-inflammatory effects of QUE.

TLR4-mediated signaling links innate and adaptive immunity, and activation of TLR4 drives and promotes inflammation (32). When TLR4 is activated, it binds to MyD88, which further activates IRAK4, ultimately leading to NF-κB activation and the release of inflammatory cytokines and chemokines, causing inflammation (32,33). Cheng *et al* (34) showed that QUE attenuated LPS-induced inflammatory damage by inducing the microRNA-21/deleted in malignant brain tumors 1/NF-κB axis. Therefore, it may serve as a potential compound for the treatment of AR. Shams and Eissa (35) showed that QUE ameliorated ethanol-induced gastric ulcers in rats, involving the nuclear factor erythroid 2-related factor 2/heme oxygenase-1, high mobility group box 1/TLR4/NF-κB pathways, suggesting that QUE possesses antioxidant and anti-inflammatory functions. Gong *et al* (36) showed that QUE attenuated LPS-induced cellular damage and inflammation via the TLR4/NF-κB pathway. The results of the present study showed that the relative expression of proteins involved in the TLR4/MyD88/IRAK4 signaling pathway was significantly increased in the OVA-induced mouse model, suggesting that inflammation in AR may be associated with this signaling pathway. The expression of these proteins was reduced in QUE-treated mice, indicating that QUE can suppress the expression of related proteins in the TLR4/MyD88/IRAK4 signaling pathway during AR inflammation. The mRNA expression levels of members of the TLR4/MyD88/IRAK4 signaling pathway were also assessed, and the changes were consistent with those obtained using western blotting. This suggests a consistent effect of QUE on related proteins and mRNAs in the TLR4/MyD88/IRAK4 signaling pathway and further supports the evidence that QUE exerts a beneficial effect on AR via this pathway.

The immune responses mediated by Th17 cells and Tregs contribute to the pathogenesis of AR (37). Th17 cells and Tregs represent two distinct phenotypes of $CD4^{+}$ T cells with completely different functions. Th17 cells have

pro-inflammatory effects, while Tregs suppress inflammation; changes in inflammatory cytokine levels can affect the Th17/Treg balance (38). Th17 cells and Tregs antagonize each other's function and differentiation, and an imbalance between Th17/Treg cells can lead to inflammatory responses, which in turn can induce AR (39,40). QUE has been reported to increase Tregs and decrease Th17 cells, thereby exerting anti-inflammatory effects (41), and its regulatory effect on Tregs may be mediated by FOXP3 (10). QUE also inhibits NF-κB activation and the release of inflammatory mediators, thereby exerting anti-allergic effects (42). Ke *et al* (31) showed that QUE improved the Treg/Th17 cell imbalance and inhibited the activation of the NF-κB pathway to treat AR. The results of the present study showed that in the OVA-induced mouse model, the percentage of Tregs in splenocytes decreased, while the percentage of Th17 cells increased, suggesting that OVA can decrease Tregs and increase Th17 cells. The Treg percentage was increased, and Th17 percentage was decreased in the spleen after QUE treatment, suggesting that QUE can reduce the number of Th17 cells and reverse the abnormally downregulated Treg population in splenocytes induced by OVA. Therefore, it is hypothesized that QUE alleviates AR by restoring the balance between Treg/Th17 cells, and that AR can be treated by correcting this imbalance.

In the present study, notable allergic symptoms were not observed in the NC group, which received only saline solution. Although QUE is as effective as DEX, long-term use of DEX can lead to side effects such as immunosuppression and metabolic disorders. By contrast, QUE is a naturally occurring flavonoid compound with a good safety profile and low toxicity. This suggests that QUE may serve as a safer natural alternative for treating AR, though further clinical validation is needed. Assessing the effect of QUE in knockout mice may be more convincing for its mechanism of action in treating AR through the TLR4/MyD88/IRAK4 signaling pathway. This should be validated through further experiments, which will be instructive for the development of QUE as a drug to prevent AR. Furthermore, the present study examined only the effects of QUE on female mice. The potential deviations in the experimental results warrant the necessity of future studies that use male mice or conduct experiments involving both male and female mice simultaneously.

In conclusion, QUE can effectively alleviate scratching and sneezing symptoms in the OVA-induced mouse model, reduce OVA-induced nasal mucosal damage, reduce the expression levels of inflammatory factors and regulate the imbalance between Treg/Th17 cells. Its mechanism of action may include reducing the inflammatory response via the TLR4/MyD88/IRAK4 signaling pathway and inducing immune tolerance. The present study primarily evaluated the therapeutic effects of QUE on AR, but its toxicity and side effects were not explored in additional depth. In addition, the small sample size used is a limitation. Whether QUE still has this effect with a larger sample size needs further verification through additional independent experiments. Therefore, it is necessary to conduct experiments with larger sample sizes to observe the therapeutic, toxic and side effects of QUE on AR in future studies.

Acknowledgements

Not applicable.

Funding

The present work was supported by grants Natural Science Foundation of China (grant nos. 81700888, 82260475 and 81860475), Guangdong Basic and Applied Basic Research Foundation (grant no. 2021A1515010971), Shenzhen Science and Technology Program for Basic Research (grant no. JCYJ20220531091417040), Shenzhen Science and Technology Program (grant no. JCYJ20210324142207019), Science and Technology Development Special Fund of Shenzhen Longgang District (grant nos. LGKCYLWS2019000864 and LGKCZSYS2019000046), Science and Technology Innovation Special-Technology Tackling Project of Shenzhen Longgang District (grant no. LGKCYLWS2022032) and Science and Technology Plan of Shenzhen Longgang District (grant no. LGKCYLWS2022003).

Availability of data and materials

The data generated in the present study may be requested from the corresponding author.

Authors' contributions

CK conceptualized the present study, performed the experiments, organized the data and prepared the original draft. JL conducted formal analysis and investigation, and participated in data analysis and interpretation. SQ participated in conceptualization and design, supervised the research process, validated the results and provided funding. XW conceptualized the study, participated in data interpretation, and critically reviewed the manuscript for important intellectual content. All authors reviewed and edited the manuscript and approved the final version of the manuscript. SQ and JL confirm the authenticity of all the raw data.

Ethics approval and consent to participate

The present study was conducted in accordance with the ARRIVE guidelines for animal research and complied with its regulations. All experimental protocols used in the study complied with animal ethics standards and were approved by the Experimental Animal Ethics Committee of Shenzhen Institute of Otorhinolaryngology (approval no. 2022-0426). All experimental methods and steps complied with relevant institutional, regional and national guidelines and regulations and the suffering to the animals was minimized as much as possible.

Patient consent for publication

Not applicable.

Competing interests

The authors declare that they have no competing interests.

References

1. Bousquet J, Anto JM, Bachert C, Baiardini I, Bosnic-Anticevich S, Walter Canonica G, Melén E, Palomares O, Scadding GK, Togias A and Toppila-Salmi S: Allergic rhinitis. Nat Rev Dis Primers 6: 95, 2020.
2. Greiner AN, Hellings PW, Rotiroti G and Scadding GK: Allergic rhinitis. Lancet 378: 2112-2122, 2011.
3. Kirtland ME, Tsitoura DC, Durham SR and Shamji MH: Toll-like receptor agonists as adjuvants for allergen immunotherapy. Front Immunol 11: 599083, 2020.
4. Murrison LB, Brandt EB, Myers JB and Hershey GKK: Environmental exposures and mechanisms in allergy and asthma development. J Clin Invest 129: 1504-1515, 2019.
5. Waage J, Standl M, Curtin JA, Jessen LE, Thorsen J, Tian C, Schoettler N; 23andMe Research Team; AAGC collaborators; Flores C, et al: Genome-wide association and HLA fine-mapping studies identify risk loci and genetic pathways underlying allergic rhinitis. Nat Genet 50: 1072-1080, 2018.
6. Shen P, Lin W, Deng X, Ba X, Han L, Chen Z, Qin K, Huang Y and Tu S: Potential implications of quercetin in autoimmune diseases. Front Immunol 12: 689044, 2021.
7. Manzoor MF, Hussain A, Sameen A, Sahar A, Khan S, Siddique R, Aadil RM and Xu B: Novel extraction, rapid assessment and bioavailability improvement of quercetin: A review. Ultrason Sonochem 78: 105686, 2021.
8. Deng Y, Shen L, Zhu H, Zhou Y and Hu X: Network pharmacology analysis of the Huangqi-Gancao herb pair reveals quercetin as a therapeutics for allergic rhinitis via the RELA-regulated IFNG/IRF1 axis response. Naunyn Schmiedebergs Arch Pharmacol 398: 1597-1612, 2025.
9. Cheng J, Zhang M, Zheng Y, Wang J and Wang Q: Integrative analysis of network pharmacology and proteomics to identify key targets of Tuomin-Zhiti-Decoction for allergic rhinitis. J Ethnopharmacol 296: 115448, 2022.
10. Lv Z, Pan Z, Huang Y, Yang H and Li X: Quercetin exhibits multi-target anti-allergic effects in animal models: A systematic review and meta-analysis of preclinical studies. Front Pharmacol 16: 1673712, 2025.
11. Yang S, Zhang J, Wang S, Zhao X and Shi J: SOCS2 overexpression alleviates diabetic nephropathy in rats by inhibiting the TLR4/NF-κB pathway. Oncotarget 8: 91185-91198, 2017.
12. Zhang Y and Zeng Y: Curcumin reduces inflammation in knee osteoarthritis rats through blocking TLR4 /MyD88/NF-κB signal pathway. Drug Dev Res 80: 353-359, 2019.
13. Yamatomo T, Okano M, Ono T, Nakayama E, Yoshino T, Satoskar AR, Harn DA Jr and Nishizaki K: Sex-related differences in the initiation of allergic rhinitis in mice. Allergy 56: 525-531, 2001.
14. Fang S, Li X, Wei X, Zhang Y, Ma Z, Wei Y and Wang W: Beneficial effects of hydrogen gas inhalation on a murine model of allergic rhinitis. Exp Ther Med 16: 5178-5184, 2018.
15. Ryu G, Bae JS, Kim JH, Kim EH, Chung YJ and Mo JH: Sneezing and rubbing counts in allergic rhinitis mouse models are a reliable indicator of type 2 immune response. Clin Exp Otorhinolaryngol 13: 308-311, 2020.
16. Livak KJ and Schmittgen TD: Analysis of relative gene expression data using real-time quantitative PCR and the 2(-Delta Delta C(T)) method. Methods 25: 402-408, 2001.
17. Okumo T, Furuta A, Kimura T, Yusa K, Asano K and Sunagawa M: Inhibition of angiogenic factor productions by quercetin in vitro and in vivo. Medicines (Basel) 8: 22, 2021.
18. Edo Y, Otaki A and Asano K: Quercetin enhances the thioredoxin production of nasal epithelial cells in vitro and in vivo. Medicines (Basel) 5: 124, 2018.
19. Cheng L, Chen J, Fu Q, He S, Li H, Liu Z, Tan G, Tao Z, Wang D, Wen W, *et al*: Chinese society of allergy guidelines for diagnosis and treatment of allergic rhinitis. Allergy Asthma Immunol Res 10: 300-353, 2018.
20. Hofmann MA, Fluhr JW, Ruwwe-Glösenkamp C, Stevanovic K, Bergmann KC and Zuberbier T: Role of IL-17 in atopy-A systematic review. Clin Transl Allergy 11: e12047, 2021.
21. Wang HR, Wei SZ, Song XY, Wang Y, Zhang WB, Ren C, Mou YK and Song XC: IL-1β and allergy: Focusing on Its role in allergic rhinitis. Mediators Inflamm 2023: 1265449, 2023.
22. Kato A: Group 2 innate lymphoid cells in airway diseases. Chest 156: 141-149, 2019.
23. Busse WW, Kraft M, Rabe KF, Deniz Y, Rowe PJ, Ruddy M and Castro M: Understanding the key issues in the treatment of uncontrolled persistent asthma with type 2 inflammation. Eur Respir J 58: 2003393, 2021.
24. Shao JB, Luo XQ, Wu YJ, Li MG, Hong JY, Mo LH, Liu ZG, Li HB, Liu DB and Yang PC: Histone deacetylase 11 inhibits interleukin 10 in B cells of subjects with allergic rhinitis. Int Forum Allergy Rhinol 8: 1274-1283, 2018.
25. Marefati N, Ghorani V, Shakeri F, Boskabady M, Kianian F, Rezaee R and Boskabady MH: A review of anti-inflammatory, antioxidant, and immunomodulatory effects of Allium cepa and its main constituents. Pharm Biol 59: 287-302, 2021.
26. Jafarinia M, Sadat Hosseini M, Kasiri N, Fazel N, Fathi F, Ganjalikhani Hakemi M and Eskandari N: Quercetin with the potential effect on allergic diseases. Allergy Asthma Clin Immunol 16: 36, 2020.
27. Ding Y, Che D, Li C, Cao J, Wang J, Ma P, Zhao T, An H and Zhang T: Quercetin inhibits Mrgprx2-induced pseudo-allergic reaction via PLCγ-IP3R related Ca^{2+} fluctuations. Int Immunopharmacol 66: 185-197, 2019.
28. Liu Y, Sha J, Meng C and Zhu D: Mechanism of lower airway hyperresponsiveness induced by allergic rhinitis. J Immunol Res 2022: 4351345, 2022.
29. Okubo K, Kurono Y, Ichimura K, Enomoto T, Okamoto Y, Kawauchi H, Suzaki H, Fujieda S and Masuyama K; Japanese Society of Allergology: Japanese guidelines for allergic rhinitis 2020. Allergol Int 69: 331-345, 2020.
30. Meng L, Qu X, Tao P, Dong J and Guo R: Quercetin alleviates the progression of chronic rhinosinusitis without nasal polyps by inhibiting nasal mucosal inflammation and epithelial apoptosis. Mol Biotechnol 67: 3532-3543, 2025.
31. Ke X, Chen Z, Wang X, Kang H and Hong S: Quercetin improves the imbalance of Th1/Th2 cells and Treg/Th17 cells to attenuate allergic rhinitis. Autoimmunity 56: 2189133, 2023.
32. Zamyatina A and Heine H: Lipopolysaccharide recognition in the crossroads of TLR4 and caspase-4/11 mediated inflammatory pathways. Front Immunol 11: 585146, 2020.
33. Bruno K, Woller SA, Miller YI, Yaksh TL, Wallace M, Beaton G and Chakravarthy K: Targeting toll-like receptor-4 (TLR4)-an emerging therapeutic target for persistent pain states. Pain 159: 1908-1915, 2018.
34. Cheng J, Luo XQ and Chen FS: Quercetin attenuates lipopolysaccharide-mediated inflammatory injury in human nasal epithelial cells via regulating miR-21/DMBT1/NF-κB axis. Immunopharmacol Immunotoxicol 44: 7-16, 2022.
35. Shams SGE and Eissa RG: Amelioration of ethanol-induced gastric ulcer in rats by quercetin: Implication of Nrf2/HO1 and HMGB1/TLR4/NF-κB pathways. Heliyon 8: e11159, 2022.
36. Gong X, Huang Y, Ma Q, Jiang M, Zhan K and Zhao G: Quercetin alleviates lipopolysaccharide-induced cell damage and inflammation via regulation of the TLR4/NF-κB pathway in bovine intestinal epithelial cells. Curr Issues Mol Biol 44: 5234-5246, 2022.
37. Mu D, Zhou L, Shi L, Liu T, Guo Y, Chen H, Luo H, Ma J, Zhang H, Xiong P and Tian L: Quercetin-crosslinked chitosan nanoparticles: A potential treatment for allergic rhinitis. Sci Rep 14: 4021, 2024.
38. Zhang S, Gang X, Yang S, Cui M, Sun L, Li Z and Wang G: The alterations in and the role of the Th17/Treg balance in metabolic diseases. Front Immunol 12: 678355, 2021.
39. Shan J, Jin H and Xu Y: T cell metabolism: A new perspective on Th17/Treg cell imbalance in systemic lupus erythematosus. Front Immunol 11: 1027, 2020.
40. Chen Z, Ke X, Wang X, Kang H and Hong S: LncRNA JPX contributes to Treg/Th17 imbalance in allergic rhinitis via targeting the miR-378g/CCL5 axis. Immunopharmacol Immunotoxicol 44: 519-524, 2022.
41. Zarenezhad E, Abdulabbas HT, Kareem AS, Kouhpayeh SA, Barbaresi S, Najafipour S, Mazarzaei A, Sotoudeh M and Ghasemian A: Protective role of flavonoids quercetin and silymarin in the viral-associated inflammatory bowel disease: An updated review. Arch Microbiol 205: 252, 2023.
42. Mlcek J, Jurikova T, Skrovankova S and Sochor J: Quercetin and its anti-allergic immune response. Molecules 21: 632, 2016.